PROCEEDINGS OF SPIE

SPIEDigitalLibrary.org/conference-proceedings-of-spie

Register cardiac fiber orientations from 3D DTI volume to 2D ultrasound image of rat hearts

Xulei Qin, Silun Wang, Ming Shen, Xiaodong Zhang, Stamatios Lerakis, et al.

Xulei Qin, Silun Wang, Ming Shen, Xiaodong Zhang, Stamatios Lerakis, Mary B. Wagner, Baowei Fei, "Register cardiac fiber orientations from 3D DTI volume to 2D ultrasound image of rat hearts," Proc. SPIE 9415, Medical Imaging 2015: Image-Guided Procedures, Robotic Interventions, and Modeling, 94152M (18 March 2015); doi: 10.1117/12.2082317

SPIE.

Event: SPIE Medical Imaging, 2015, Orlando, Florida, United States

Register cardiac fiber orientations from 3D DTI volume to 2D ultrasound image of rat hearts

Xulei Qin [1], Silun Wang [2], Ming Shen [3], Xiaodong Zhang [2],
Stamatios Lerakis [3,1], Mary B. Wagner [4], Baowei Fei [1,5]*

[1]*Department of Radiology and Imaging Sciences, Emory University, Atlanta, GA*
[2] *Yerkes National Primate Research Center, Emory University, Atlanta, GA*
[3] *Division of Cardiology, Department of Medicine, Emory University, Atlanta, GA*
[4] *Department of Pediatrics, Emory University, Atlanta, GA*
[5]*Department of Biomedical Engineering, Emory University and Georgia Institute of Technology, Atlanta, GA*
**E-mail: bfei@emory.edu; web: http://feilab.org*

ABSTRACT

Two-dimensional (2D) ultrasound or echocardiography is one of the most widely used examinations for the diagnosis of cardiac diseases. However, it only supplies the geometric and structural information of the myocardium. In order to supply more detailed microstructure information of the myocardium, this paper proposes a registration method to map cardiac fiber orientations from three-dimensional (3D) magnetic resonance diffusion tensor imaging (MR-DTI) volume to the 2D ultrasound image. It utilizes a 2D/3D intensity based registration procedure including rigid, log-demons, and affine transformations to search the best similar slice from the template volume. After registration, the cardiac fiber orientations are mapped to the 2D ultrasound image via fiber relocations and reorientations. This method was validated by six images of rat hearts *ex vivo*. The evaluation results indicated that the final Dice similarity coefficient (DSC) achieved more than 90% after geometric registrations; and the inclination angle errors (IAE) between the mapped fiber orientations and the gold standards were less than 15 degree. This method may provide a practical tool for cardiologists to examine cardiac fiber orientations on ultrasound images and have the potential to supply additional information for diagnosis of cardiac diseases.

Keywords: Cardiac fiber orientation; ultrasound imaging; magnetic resonance diffusion tensor imaging (MR-DTI); 2D/3D registration, echocardiography

1. INTRODUCTION

Two-dimensional (2D) cardiac ultrasound imaging or echocardiography is one of the most convenient and routine imaging modality in cardiology because it is non-invasive, lack of radiation, inexpensive and fast for dynamic imaging [1]. It can supply the information for the diagnosis of the mass and shape of the heart, pumping capacity, and systolic/diastolic functions. Generally, these parameters only supply the pathological deformation of the myocardial geometries or structures [2]. On the other hand, cardiac fibers are the basic structural, mechanical, and electrophysiological units to generate the diastolic or systolic cycle and to pump the bloods from the ventricles into the circulation [3]. Particularly, the cardiac fiber orientation plays an important role in determining the stress distribution within the cardiac walls and in determining the electrical activation spreading during beating periods [4, 5]. Registering cardiac fiber orientations from magnetic resonance diffusion tensor imaging (MR-DTI) to ultrasound images may supply more detailed microstructure information of the myocardium [6-8]. This could also help cardiologists to better understand the cardiac physiology and have the potential to supply new information for the diagnosis of cardiac diseases.

Medical Imaging 2015: Image-Guided Procedures, Robotic Interventions, and Modeling,
edited by Ziv R. Yaniv, Robert J. Webster III, Proc. of SPIE Vol. 9415, 94152M
 · doi: 10.1117/12.2082317

Currently, MR-DTI has been utilized to extract the fiber orientations of cardiac fibers because of its ability in measuring the diffusion tensors of the water in biological tissue [9-14]. Unfortunately, this imaging is very time consuming and have severe artifacts during *in vivo* cardiac imaging. It can image three-dimensional (3D) fiber orientations at a high resolution *ex vivo*. The aim of this study is to register cardiac fiber orientations from a 3D MR-DTI volume to 2D ultrasound images. This 2D/3D registration problem has been investigated for other purposes in our group [15,19]. Huang *et al.* proposed a method to register dynamic 2D dynamic ultrasound image and 3D preoperative CT volume for cardiac invasive surgeries [16]. Both spatial and temporal registrations are used to map images for the beating heart surgery application. For the purpose of imaged-guided therapy for prostate cancer, Fei *et al.* provided a slice-to-volume algorithm to register the live-time interventional MR 2D images to the preoperative high-resolution MR volume [17]. It could achieve high accuracies with different image noises, inhomogeneity, and artifacts. However, these registrations were between the 2D/3D images of the same objects. For our purpose, the MR-DTI data are not acquired from the same subject *in vivo* and they are from template hearts *ex vivo* instead. Then, the previous methods could not be directly applied here because both 2D ultrasound images and 3D MR-DTI volumes are from different hearts.

Therefore, in this project, we propose a registration method to map cardiac fiber orientations from a 3D MR-DTI volume to 2D ultrasound images. First, for the template heart, its geometry and fiber orientations are imaged by ultrasound and DTI in the short-axis, respectively. They are registered and fused into one volume as the template, which includes both ultrasound intensity and fiber orientations. Second, the target 2D ultrasound image is registered to the template volume to search for the best matching slice via rigid and non-rigid registrations. Finally, according the deformation field derived from the registration, the cardiac fiber orientations of the best matching slice from the template volume are inversely deformed as the mapped results of the target 2D ultrasound image. The method, experimental design and its evaluation are described in the following sections.

2. Methods

In this study, we used an intensity based registration approach. The whole procedure of registering cardiac fiber orientations from the 3D MR-DTI volume to the 2D ultrasound image is illustrated in Figure 1. We use the ultrasound images that were acquired in the short-axis view. After data acquisitions, the 3D volume of the template heart is reconstructed, which includes both ultrasound intensities and DTI fiber orientations. Then, for a target 2D ultrasound image form another heart, its geometry is first registered to the template volume based on intensity registration and then the template fiber orientations are inversely mapped back to the ultrasound image as its results.

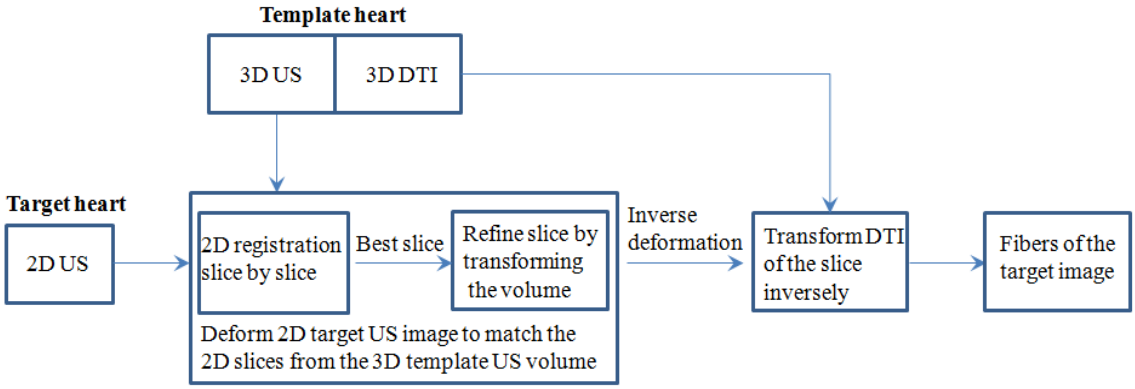

Figure 1. Flowchart of mapping cardiac fiber orientation from 3D MR-DTI to 2D ultrasound

A. Data acquisition and pre-processing

The ultrasound volumes of three fixed rat hearts were imaged by the Vevo 2100 ultrasound system (FUJIFILM

VisualSonics, Inc., Toronto, Canada) with a 30 MHz transducer. B-mode ultrasound images of the hearts in the short-axis view were acquired from apex to base, slice by slice, at a 0.2 mm thickness interval in a field of view (FOV) of 15.4×20×20 mm^3. The hearts were then imaged by a high-field Biospec 7 T MR scanner (Bruker Corporation, Massachusetts, USA) using an RF coil with an inner diameter of 30 mm. Before DTI data acquisition, anatomical MR images were acquired with a voxel resolution of 0.078 mm × 0.078 mm × 0.156 mm^3. Then, the cardiac fiber orientations were imaged in 30 directions by the spin echo sequences at a 0.234 mm isotropic resolution in an FOV of 30×30×20 mm^3. Each slice was also imaged in the short-axis view from the ventricular apex to the base.

After the data acquisitions, the 3D geometry of each heart was reconstructed from the MR images after semi-manually segmentation using the Analyze software (AnalyzeDirect Inc., Overland Park, USA). Then, the tensors of DTI data were decomposed into three eigenvectors and cardiac fiber orientations were tracked by a determinative method of fractional anisotropy. Both ultrasound and DTI volumes are fused in one template volume.

B. Geometric registration and fiber orientation deformation

Slice-by-slice searching

As the 2D ultrasound and 3D template slices are all in the short-axis view, the first step is to find the first similar slice of the volume via slice-by-slice searching. In this step, the 2D ultrasound image (I_{US}) is registered to each slice of the template volume by a rigid registration followed by the log-Demons registration [18] based on ultrasound intensities. Rigid registration is based on the sum of the intensity squares and the log-Demons registration is stopped for each slice after 200 iteration or the consistent errors is lower than 10^{-4}. Then, the most similar slice (S_1) of the volume is chosen with the maximum mutual information between the slice and its registered image (I_1). For the given target image (T) and the reference image (R), their mutual information is defined as follows [19-22]:

$$MI(T,R) = \sum_{t,r} p_{T,R}(t,r) log \frac{p_{T,R}(t,r)}{p_T(t) \cdot p_R(r)}, \quad (1)$$

Here, $p_{T,R}(t,r)$ is the joint probability, $p_T(t)$ and $p_R(r)$ are both marginal probabilities of the intensity histograms of both images. The corresponding transformation fields are set as: T_1 for rigid registration and T_2 for log-demons registration.

Neighbor space searching

After the S_1 searching, another affine registration is applied to the template volume to search the final best slice in the neighbor space of S_1. Though all images are supposed in the short-axis view, the real acquisitions may have some transformation. The affine transform does not consider the shear transformation. During the affine transform searching process, the transform is initialized as an identity matrix. It is optimized by a nonlinear least-squares optimizer in MATLAB 2013a (The MathWorks, Inc., Natick, MA). The similarity criterion is the square differences between I_1 and the corresponding slice from the transformed volume. After 200 iteration or the consistent error is lower than 10^{-4}, the optimization process stops. Its searching slice is defined as S_2 and its corresponding affine transformation is T_3.

Cardiac fiber relocation and reorientation

After intensity based geometry registrations, the corresponding transform matrixes T_1, T_2, and T_3 are applied to relocate the cardiac fiber orientations (F). Here T_1 and T_2 are inversely utilized. For the fiber orientations, the rigid and affine transformation follows the preservation of principal direction (PPD) method [23]. Here, the fiber orientations are represented by the first eigenvectors of the MR-DTI data. Moreover, this method can also be extended to the deformable transformations by an approximate affine transformation $A = Id + J(T_2)$ where Id is the identity matrix and J is the Jacobian matrix. Then, the mapped fiber orientations for 2D ultrasound image can be written as:

$$F' = \frac{T_1^{-1} \cdot T_2^{-1} \cdot T_3 \cdot F}{\left\| T_1^{-1} \cdot T_2^{-1} \cdot T_3 \cdot F \right\|} \quad (2)$$

C. Evaluations

Various evaluation methods have been used to validate image registration [20, 24-30]. The first quantitative evaluation of the volume registration is conducted by comparing the registered volume with the corresponding target volume. The Dice similarity coefficient (DSC) is used as the performance assessment score of the similarity between both volumes. It is computed as follows:

$$DSC(R,S) = \frac{2Volum(R \bigcap S)}{Volum(R) + Volum(S)}, \quad (3)$$

where R and S represent the voxel set in the volumes of both registered volume and the corresponding target volume, respectively.

In order to evaluate the extracted cardiac fiber orientations, both estimated orientation and the gold standard in the same voxels are compared by two parameters: the acute angle error (AAE) and the inclination angle error (IAE). The acute angle is utilized to measure the angular separation between both orientations of the same fiber by inverting the absolute of their dot product in 3D into an angle [23, 31].

3. Results

3.1 Registration results on ultrasound volumes

We evaluated the registration method using 6 ultrasound images from rat hearts. Their template volumes were from different hearts. The geometry registration and cardiac fiber orientations mapping results were evaluated by the three parameters of DSC, AAE and IAE.

The procedure of the geometry registration and its typical result are shown in Figure 2. Figure 2(a) is the 2D target ultrasound image that needs to be registered to a 3D volume of the template heart with known fiber orientations. In the first step, the target slice was quickly registered to each slice of the 3D volume of the template heart. Figure 2(b) indicates the result after a rough rigid registration slice-by-slice to find the most similar one in the 3D volume of the template heart. After that, the rigid registered target slice was deformed to match the geometry of the selected 3D volume slice. Figure 2(c) is the result after log-demons registration to the selected slice in the 3D volume of the template heart by the step in Figure 2(b). The 3D template volume was then optimized via an affine transform to find the best matching slice for (c). Based on the optimization, the inversely transformed result of (c) is shown in Figure 2(d). For comparison, the fusion result of both deformed image of the 2D slice and the corresponding 2D image in the 3D volume are shown in Figure 2(f).

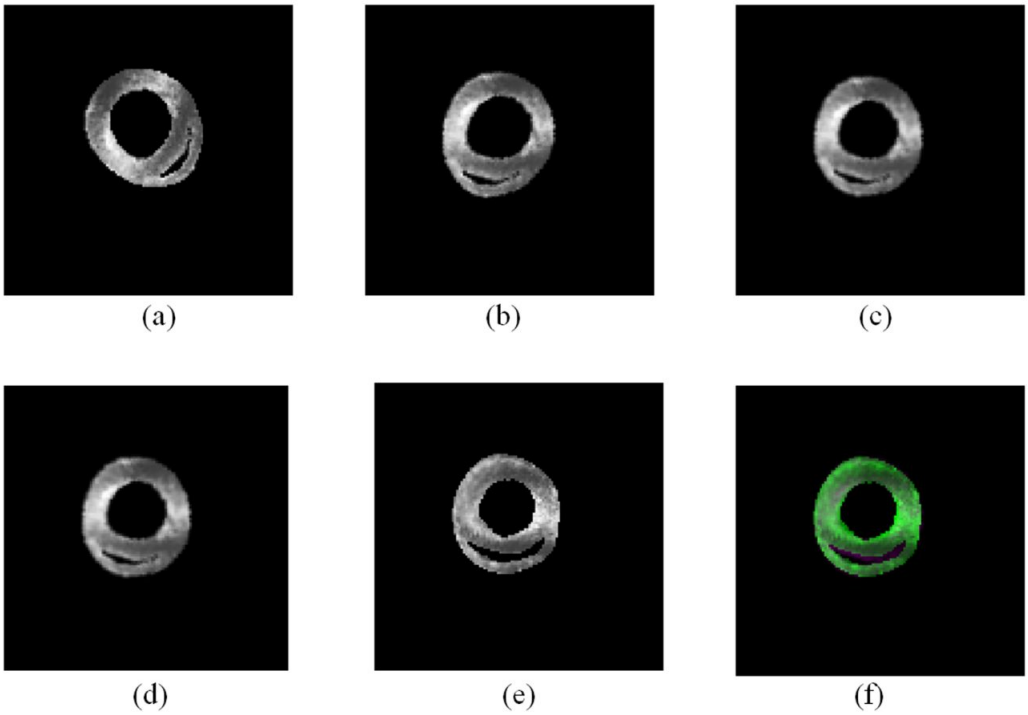

Figure 2. Example results of the image registration and inverse transformations. (a) Input 2D ultrasound image. (b) Result of the 2D image after rigid registration slice by slice from the 3D template volume. (c) Result after log-demons registration. (d) Result after affine registration inversely. (e) Corresponding slice in the volume. (f) Fusion of (d) and (e).

3.2 The inverse deformation of cardiac fiber orientation

After geometric registration, the cardiac fiber orientations were registered from the template heart to the 2D target ultrasound image based on the geometric registration matrix. The cardiac fiber orientation of the template heart was imaged by high-resolution MR-DTI *ex vivo*. The results of the cardiac fiber orientations estimation are shown in Figure 3. Figure 3(a) presents the fiber orientations in a 2D slice selected from the template heart and three images correspond to three different fiber directions. Figure 3(b) indicates the fiber orientations estimated for the target 2D slice, which is based on the deformation field derived from the geometric registration. These estimated fiber orientations can be compared with the real ones imaged by MR-DTI shown in Figure 3(c).

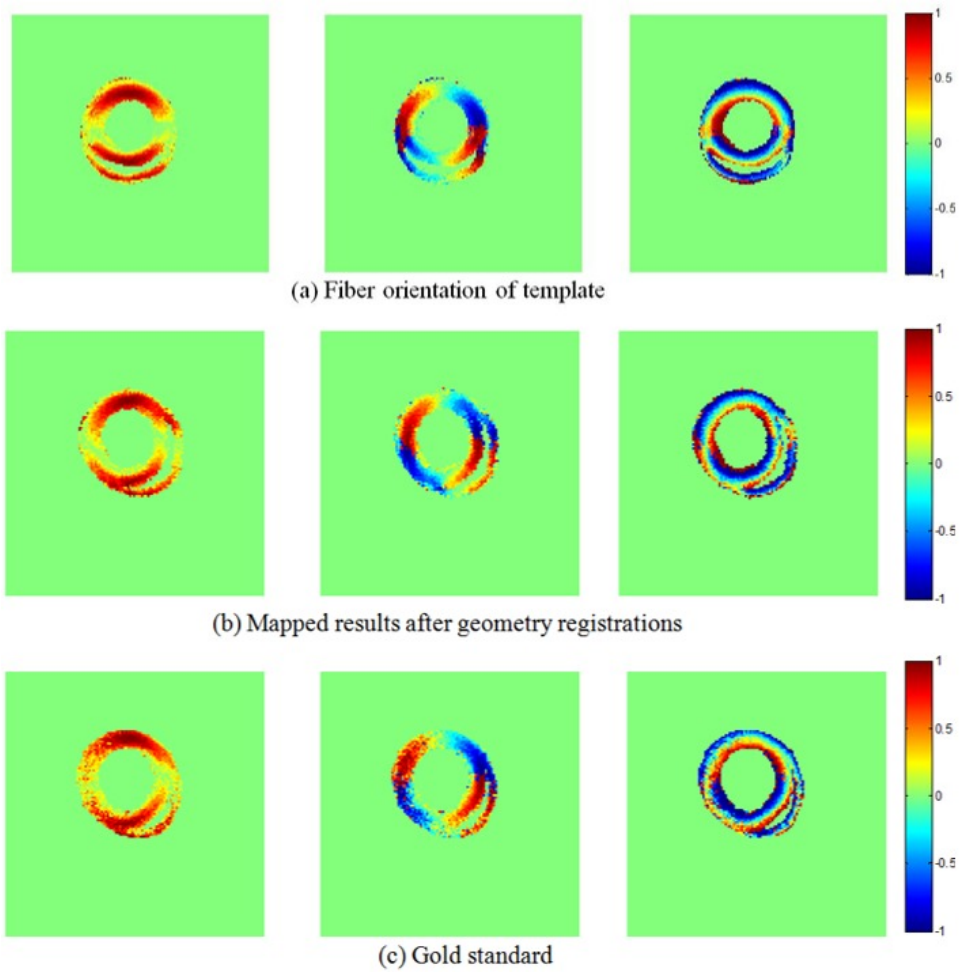

Figure 3. Registered cardiac fiber orientations from DTI volume to 2D ultrasound geometry. (a) DTI fiber orientations. (b) Mapped results after geometric deformations. (c) Gold standard.

In order to quantitatively compare the estimated fiber orientations with the real one from MRI-DTI, both geometric registration and cardiac fiber mapping of 6 images were evaluated by DSC, AAE and IAE, respectively. These results indicate that after rigid registration the mean DSC was 83.0±5.5%. After deformable registration it increased to 92.5±1.7%. After the multi-step geometry registration, the fiber orientations were estimated. The mean AAE was 30.1±1.2 degree and the mean IAE was 13.3±0.6 degree. The detailed results were shown in Table 1.

Table 1. The evaluation results of both geometric registrations and mapped cardiac fiber orientations from template volumes to target images.

Imaging Data		Rigid DSC (%)	Final DSC (%)	AAE (degree)	IAE (degree)
Target image	Template				
Image 1 of Rat 1	Rat 2 volume	84.0	91.7	28.8	14.1
Image 2 of Rat 1	Rat 2 volume	89.9	91.3	29.8	13.2
Image 3 of Rat 1	Rat 2 volume	85.7	90.4	29.1	13.3
Image 1 of Rat 3	Rat 1 volume	81.9	93.0	30.1	12.3
Image 2 of Rat 3	Rat 1 volume	73.3	94.9	30.7	13.7
Image 3 of Rat 3	Rat 1 volume	83.4	93.7	32.2	13.4
Mean ± Standard Deviation		83.0±5.5	92.5±1.7	30.1±1.2	13.3±0.6

4. Conclusions

We investigated the registration between cardiac fiber orientations from a 3D MR-DTI volume and 2D ultrasound images. The fiber orientations of the 3D DTI were imaged *ex vivo* and the 2D ultrasound images were acquired *in vivo*. Based on our proposed procedure, the fiber orientations could be mapped to the 2D imaged ultrasound images in clinical applications. This method may supply additional information for the cardiac diagnosis using 2D ultrasound images.

ACKNOWLEDGMENT

This research is supported in part by NIH grants R21CA176684, R01CA156775 and P50CA128301, Georgia Cancer Coalition Distinguished Clinicians and Scientists Award, and the Center for Systems Imaging (CSI) of Emory University School of Medicine.

REFERENCES

[1] X. Qin, L. Wu, H. Jiang *et al.*, "Measuring body-cover vibration of vocal folds based on high frame rate ultrasonic imaging and high-speed video," IEEE Trans Biomed Eng, 58(8), 2384 - 2390 (2011).

[2] X. Qin, Z. Cong, and B. Fei, "Automatic segmentation of right ventricular ultrasound images using sparse matrix transform and level set," Physics in Medicine and Biology 58(21), 7609-24 (2013).

[3] T. Arts, F. W. Prinzen, L. H. Snoeckx *et al.*, "Adaptation of cardiac structure by mechanical feedback in the environment of the cell: a model study," Biophysical Journal, 66(4), 953-61 (1994).

[4] P. P. Sengupta, J. Korinek, M. Belohlavek *et al.*, "Left ventricular structure and function: basic science for cardiac imaging," J Am Coll Cardiol, 48(10), 1988-2001 (2006).

[5] P. P. Sengupta, V. K. Krishnamoorthy, J. Korinek *et al.*, "Left ventricular form and function revisited: applied translational science to cardiovascular ultrasound imaging," J Am Soc Echocardiogr, 20(5), 539-51 (2007).

[6] X. Qin, Z. Cong, R. Jiang *et al.*, "Extracting cardiac myofiber orientations from high frequency ultrasound images " Proceedings of SPIE, 8675, 867507-8 (2013).
[7] X. Qin, and B. Fei, "Measuring myofiber orientations from high-frequency ultrasound images using multiscale decompositions," Phys Med Biol, 59(14), 3907-3924 (2014).
[8] X. Qin, S. Wang, M. Shen *et al.*, "Mapping cardiac fiber orientations from high resolution DTI to high frequency 3D ultrasound," Proceedings of SPIE, 9036, 90361 (2014).
[9] L. Geerts-Ossevoort, P. Bovendeerd, F. Prinzen *et al.*, "Myofiber orientation in the normal and infarcted heart, assessed with MR-diffusion tensor imaging," Computers in Cardiology 2001, 28, 621-624 (2001).
[10] L. Geerts, P. Bovendeerd, K. Nicolay *et al.*, "Characterization of the normal cardiac myofiber field in goat measured with MR-diffusion tensor imaging," Am J Physiol Heart Circ Physiol, 283(1), H139-45 (2002).
[11] M. T. Wu, W. Y. I. Tseng, M. Y. M. Su *et al.*, "Diffusion tensor magnetic resonance imaging mapping the fiber architecture remodeling in human myocardium after infarction - Correlation with viability and wall motion," Circulation, 114(10), 1036-1045 (2006).
[12] H. Lombaert, J. M. Peyrat, P. Croisille *et al.*, "Human atlas of the cardiac fiber architecture: study on a healthy population," IEEE Trans Med Imaging, 31(7), 1436-47 (2012).
[13] P. Savadjiev, G. J. Strijkers, A. J. Bakermans *et al.*, "Heart wall myofibers are arranged in minimal surfaces to optimize organ function," Proc Natl Acad Sci U S A, 109(24), 9248-53 (2012).
[14] F. Vadakkumpadan, H. Arevalo, C. Ceritoglu *et al.*, "Image-based estimation of ventricular fiber orientations for personalized modeling of cardiac electrophysiology," IEEE Trans Med Imaging, 31(5), 1051-60 (2012).
[15] H. S. Wang, and B. W. Fei, "Nonrigid point registration for 2D curves and 3D surfaces and its various applications," Physics in Medicine and Biology, 58(12), 4315-4330 (2013).
[16] X. Huang, J. Moore, G. Guiraudon *et al.*, "Dynamic 2D ultrasound and 3D CT image registration of the beating heart," IEEE Trans Med Imaging, 28(8), 1179-89 (2009).
[17] B. W. Fei, J. L. Duerk, D. T. Boll *et al.*, "Slice-to-volume registration and its potential application to interventional MRI-guided radio-frequency thermal ablation of prostate cancer," Ieee Transactions on Medical Imaging, 22(4), 515-525 (2003).
[18] T. Vercauteren, X. Pennec, A. Perchant *et al.*, "Symmetric Log-Domain Diffeomorphic Registration: A Demons-Based Approach," Medical Image Computing and Computer-Assisted Intervention - Miccai 2008, Pt I, Proceedings, 5241, 754-761 (2008).
[19] B. Fei, J. L. Duerk, D. T. Boll *et al.*, "Slice-to-volume registration and its potential application to interventional MRI-guided radio-frequency thermal ablation of prostate cancer," IEEE Trans Med Imaging, 22(4), 515-25 (2003).
[20] B. Fei, C. Kemper, and D. L. Wilson, "A comparative study of warping and rigid body registration for the prostate and pelvic MR volumes," Comput Med Imaging Graph, 27(4), 267-81 (2003).
[21] B. Fei, H. Wang, R. F. Muzic, Jr. *et al.*, "Deformable and rigid registration of MRI and microPET images for photodynamic therapy of cancer in mice," Med Phys, 33(3), 753-60 (2006).
[22] G. Lu, L. V. Halig, D. Wang *et al.*, "Hyperspectral imaging for surgical margin delineation of head and neck cancer: registration of hyperspectral and histological images" Proceedings of SPIE, 9036, 9036-28 (2014).
[23] D. C. Alexander, C. Pierpaoli, P. J. Basser *et al.*, "Spatial transformations of diffusion tensor magnetic resonance images," Ieee Transactions on Medical Imaging, 20(11), 1131-1139 (2001).
[24] B. Fei, J. L. Duerk, and D. L. Wilson, "Automatic 3D registration for interventional MRI-guided treatment of prostate cancer," Comput Aided Surg, 7(5), 257-67 (2002).
[25] B. Fei, A. Wheaton, Z. Lee *et al.*, "Automatic MR volume registration and its evaluation for the pelvis and prostate," Phys Med Biol, 47(5), 823-38 (2002).
[26] X. Qin, S. Wang, and M. Wan, "Improving reliability and accuracy of vibration parameters of vocal folds based on high-speed video and electroglottography," IEEE Trans Biomed Eng, 56(6), 1744-54 (2009).
[27] I. Sechopoulos, K. Bliznakova, X. L. Qin *et al.*, "Characterization of the homogeneous tissue mixture approximation in breast imaging dosimetry," Medical Physics, 39(8), 5050-5059 (2012).
[28] G. Lu, L. V. Halig, D. Wang *et al.*, "Spectral-spatial classification using tensor modeling for head and neck cancer detection of hyperspectral imaging," Proceedings of SPIE, 9034, 903413 (2014).
[29] X. Qin, G. Lu, I. Sechopoulos *et al.*, "Breast tissue classification in digital breast tomosynthesis images based on global gradient minimization and texture features," Proceedings of SPIE, 9034, 90341-8 (2014).
[30] G. Lu, L. V. Halig, D. Wang *et al.*, "Spectral-spatial classification for noninvasive cancer detection using hyperspectral imaging," J Biomed Opt., 19(10), 106004 (2014).
[31] S. Hari Sundar, H., D. G. Shen, G. Biros *et al.*, "Estimating myocardial fiber orientations by template warping," 2006 3rd IEEE International Symposium on Biomedical Imaging: Macro to Nano, Vols 1-3, 73-76 (2006).